

The Experimental Research of NO Removal by Dielectric Barrier Discharge at Atmospheric Pressure

Yun Liu⁺, Wei Zong, Haiping Xiao, Xudong Gao, Baomin Sun and Zhongyang Chen

Key Laboratory of Condition Monitoring and Control for Power Plant Equipment (North China Electric Power University), Ministry of Education, Beijing, China

Abstract. A set of experimental set-up of coaxial cylinder-tube dielectric barrier discharge reactor is designed to investigate NO removal with non-thermal plasma produced by barrier discharges. Experimental results show that the method is effective. The influences of length of the discharge region, the discharge gap, the amplitude and frequency of applied voltage on the NO removal rate are also investigated respectively. The results show that removal rate of NO increased with increasing length of the discharge region and the power voltage. As discharge gap and power frequency increasing, the removal rate of NO increases first and then decreases.

Keywords: Dielectric barrier discharge, experimental system, NO removal rate, parameters of reactor and power supply

1. Introduction

Dielectric barrier discharge (DBD for short) is an effective method to produce low-temperature and non-equilibrium plasma. Because DBD can easily generate plasma at atmospheric pressure or above atmospheric pressure conditions, obtain activity particles required for the chemical reaction at a lower temperature without vacuum equipment, and have special light, heat, sound, electricity and other physical and chemical processes. It is used in many fields such as flue gas treatment, ozone synthesis, sewage treatment, UV light source, high-power CO₂ lasers, materials and surface modification in recent years. At present, the research of the characteristics of DBD has made some progress; however, there is a lack of knowledge about relevant parameters of DBD's mechanism, relationships and influence on evolution of discharge form as lack of effective diagnostic and measurement instruments. Further study is needed both in theory and experiment field.

2. Basic Characteristics of Dielectric Barrier Discharges

Dielectric barrier discharge is generated in discharge configuration with at least one dielectric barrier between two planar or cylindrical electrodes connected to an AC or pulse power supply. Dielectric can cover the electrode, and may also be hung in the discharge space. When the electrodes apply a certain frequency (from 50 Hz to several gigahertz) and an AC voltage whose amplitude is high enough, the gas between electrodes are breakdown resulting dielectric barrier discharge. At atmospheric pressure or above atmospheric pressure conditions, the discharges in gap are composed of a number of random distribution micro-discharge which is generally duration nanosecond [1]. Each micro-channel is a strong streamer discharge breakdown process and the transport process of charged particles and the plasma chemical reaction are taken place in these micro-discharge channels. Therefore, many researchers consider micro-discharge as the main

⁺ Corresponding author.

E-mail address: luoye861228@yahoo.com.cn.

characteristics of DBD, and research the general features of DBD by studying the characteristics of micro-discharge [2, 3, 4].

From physical process, supply voltage forms the electric field through capacitor coupling to dielectric discharge gap. Space electrons get energy from the electric field, and then non-elastic collides with surrounding gas. Through this collision, energy was transferred to the gas molecules. Electron avalanche happens when the gas is stimulated, which generates a considerable amount of space charges. Space charges superimpose on external electric field, form high local electric field. The speed of electron in discharge gap forms space charge faster than the speed of electron transfer. Conductive channels generate a large number of filamentous micro-discharges through the discharge very quickly. When the micro-discharge channel formed, space charges in the channel transport and accumulate in the medium surface, result in the reverse electric field to put discharge off, and then micro-discharge pulses are formed. Within a certain range, the number of micro-discharge increase with the increasing power supply voltage and frequency.

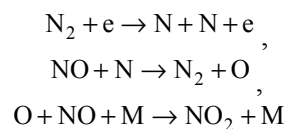
The presence of dielectric, can effectively limit the movement of charged particles, and prevent the discharge current unlimited growth, thus avoid the formation of the spark discharge within the discharge gap or arc discharge. And it also can make micro-discharge distribute uniform and stable in the entire discharge space, and easily get a large volume of low-temperature non-equilibrium plasma, so that DBD can be widely applied in industry.

The discharging and intensity mainly depend on: 1) Dielectric materials and structural elements, which mainly contain the properties of dielectric materials, dielectric constant, thickness, geometry and the distance between the discharging gap etc. 2) Source of supply elements, mostly are power supply voltage, frequency, waveform and control mode etc. 3) Externalities, mostly are the component of the working gas, pressure, the flow rate of the gas and the working temperature of DBD plasma generator etc.

3. The Mechanism of Dielectric Blocking Off the Discharging to Wipe out the NO

There are about three phrases for dielectric blocking off the discharging to wipe out the NO: 1) Current pulse phase. It lasts about dozens of ns. The characteristics of this stage is that there is active material generated when the inelastic collision occurs between electronics and neural substance; 2) the phrase of administer after the pulse. This phase lasts dozens of ns to hundreds of ps. Chemical reactions were caused after enough active material which was generated from the pulse process. They are treated out in this phrase; 3) the phase of pulse interval. The phase will last hundreds of μ s to hundreds of ms. In this stage, the concentration of NO has almost no change, but it can consume the O_3 generated from the reaction. The phases are overlapping in time and space. The component and status of the previous system of pulse interval are the foundation of next stage of current pulse, and they depend on the type and efficiency of the affection of the administer stage after pulse.

In the mixed gas of N_2 and NO, it's always considered that the remove of NO mainly depends on the chemical reaction on the atom N, and the source of atom N is the collision between high-energy electrons. The main reaction mechanism of the dielectric resisting charging to remove NO is:



and above all the M stands for the third, it may be electron, neutral particle or the photon generated from the complex process. According to the reaction mechanism above, it is favorable for the remove of NO to generate as much high-energy electron as possible.

4. The Experimental System of Remove NO by Dielectric Barrier Discharge

4.1 Dielectric barrier discharge reactor

The experiment used the reactor of the dielectric barrier discharge with the structure of coaxial cylindrical electrodes, as Fig. 1. The resisting Dielectric materials of double layers of outside and inside are quartz glass

tube. The high-voltage electrode is a stainless steel rod whose diameter is 3mm, and it is connected with the high-voltage output of the source. The grounding electrode is a copper mesh covered the medium on the outer. And it is connected with the ground terminal of the source. The medium inside and outside are both quartz. Analyzed from the structure of Physical, The dielectric barrier discharge reactor is actually a Lossy capacitor composed of discharge electrode, dielectric layer and the discharge gap. The power supply is equivalent to the equivalent circuit in Fig. 1. C is the discharge gap and dielectric equivalent capacitances. R_g is the equivalent capacitance of discharge gap which is changed as the voltage changed between the electrodes, and goes with highly nonlinear. L is the equivalent inductance.

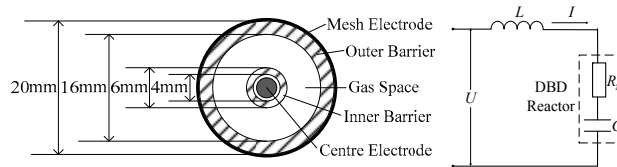
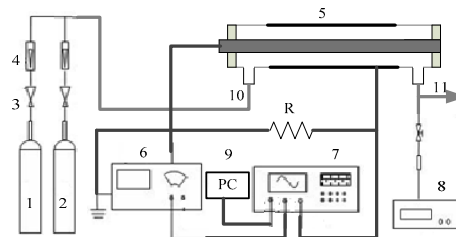


Figure 1. Reactor structure and equivalent circuit of DBD load

4.2 The experimental system

The experimental system is showed in Fig. 2. The whole can be divided into four systems: 1) Gas Distribution System It includes the NO standard gas cylinder (1.01%NO+N₂) and the high purity N₂ gas cylinder (purity>=99.999%), and some matching devices of flow control such as rotameter. 2) Power supply and waveform acquisition system. It includes standard AC power, voltage regulator, plasma generator power supply (voltage is adjustable from 0 kV to 30 kV, Frequency is adjustable from 5 kHz to 25 kHz), and the digital memory scope TDS2024 which can be used to collect voltage, current waveform. 3) DBD reactor. 4) The analysis and detection system of smoke. The portable precision gas analyzer is testo350Pro, which can be used to measure the smoke parameter of O₂, NO, NO₂, SO₂. It also can be used to measure the temperature of smoke.



1-Bottle of NO, 2-Bottle of N₂, 3-Relief valve, 4-Rotameter, 5-DBD reactor, 6-High-voltage power supply, 7-Oscilloscope, 8-Flue gas analyzing apparatus, 9-Computer, 10-Gas inlet, 11-Exhaust exit

Figure 2. Experimental set-up

5. Experimental Results and Discussion

The experimental system is used to research different length of the discharge region, various discharge gaps, supply voltage and power frequency effect on NO removal rate.

5.1 Definition

The removal rate η of NO is defined as

$$\eta = \frac{C_{in} - C_{out}}{C_{in}} \times 100\% \quad (1)$$

where C_{in} and C_{out} are NO concentrations before and after the plasma processing.

5.2 Effect of length of discharge region on removal rate of NO

Dielectric barrier discharge didn't take place uniform throughout the discharge space, but was a large number of filamentous discharge channels which appeared randomly in various locations. When discharge gap was smaller than 5mm, discharges seemed relatively uniform, and were close to the glow discharge, but not glow [5].

As discharge gap was too small, the electric field strengthened that the discharge did not change along the diameter direction at the time of discharge. The micro-discharges were random distribution in different positions, but the characteristic time was very short (about 1 ~ 10 ns) and discharge gap was small, so that the electron density in the space was evenly distributed and unchanged when discharge was sustained. NO concentration mathematical model in dielectric barrier discharge was established [6].

In NO and N₂ gas mixture, NO concentration with time varying at normal temperature and atmospheric pressure can be expressed as:

$$C_{NO} = C_{NO}^0 \exp \left\{ \frac{2\beta}{\alpha} [1 - (\alpha t + \exp(-\alpha t))] \right\}, \quad (2)$$

where α is $2.205 \times 10^9 s^{-1}$ and β is a constant. Superscript '0' is the initial value when time t is equal to zero.

Gas residence time in reactor is:

$$\tau_r = LS/Q, \quad (3)$$

where L is the length of discharge region, S is the cross-sectional area of discharge gap, Q is the gas volume flow rate. According to the size of reactor and gas flow rate used in the experiment, Calculate gas residence time in reactor τ_r is 0.4s, so $\alpha\tau_r$ is much larger than one. When superscript 'NO' is removed, equation (2) can be simplified as:

$$C = C^0 \exp(-2\beta t). \quad (4)$$

Supposed the concentration of NO is C_x at x , according to (4), the concentration at $x + \Delta x$ is:

$$C_{x+\Delta x} = C_x \exp(-2\beta\tau_r\Delta x/L), \quad (5)$$

when Δx approach to zero, $C_{x=0}$ is equal to C_{in} and x is equal to L ,

$$C_{out} = C_{in} \exp(-2\beta\tau_r). \quad (6)$$

Logarithmic on both sides of the equation:

$$\ln C_{in} - \ln C_{out} = 2\beta LS/Q. \quad (7)$$

Equation (7) shows that, when the center electrode, the size of reactor and gas flow rate is fixed, there is a linear relationship between logarithmic decrement of NO concentrations inlet and outlet and the length of discharge region. It is also shown in Fig. 3, that curve slope is larger at slow flow rate, compared two different flow rate $Q=6.3L/min$ and $Q=10.5L/min$. That is to say $\ln C_{in} - \ln C_{out}$ is direct proportion with the length of discharge region L , and is inversely proportional to flow rate Q .

Fig. 4 shows the longer discharge region, the larger NO removal rate. At low flow rate, with the length of discharge region increasing, the improving trend of NO removal rate is more and more slowly. When gas flow rate is large, the trend is less obvious.

Fig. 5 shows, the trend of NO removal rate with power increasing is coincidental at different lengths of discharge region. When power is less than 20 W, removal rate is almost same at 5 cm and 10cm, but the removal rate is smaller for length of 20 cm. NO removal rate increases with the increasing length of discharge region at the same input power, however the effect is not obvious. Therefore, the appropriate length of reactor can be chosen considering economic.

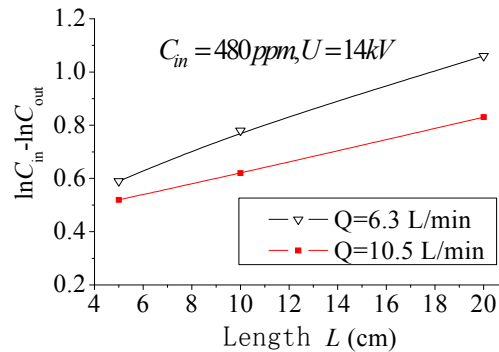


Figure 3. Relation between $\ln C_{in} - \ln C_{out}$ and length

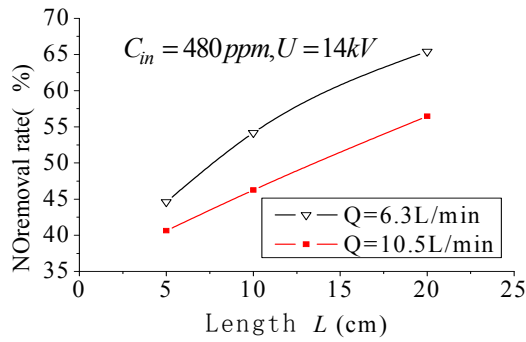


Figure 4. Relation between removal rate of NO and length

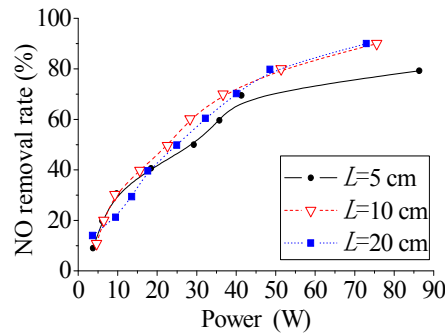


Figure 5. Relation between NO removal rate and discharge power

5.3 Effect of discharge gap on removal rate of NO

The effect of discharge gap on NO removal rate was not monotonous [7]. It was necessary to survey the influence of different gap on NO removal.

Two different discharge gaps which diameters were $\Phi 20 \times \Phi 16 + \Phi 6 \times \Phi 4$ and $\Phi 25 \times \Phi 21 + \Phi 6 \times \Phi 4$ were used in the experimental. The gas was mixed with 10L N_2 and 0.5L NO at normal temperatures and pressures. When frequency was 10 kHz and voltage rose from 0 to 5 kV, discharge phenomenon can be observed in 5 mm gas gap reactor, at the same time some NO was removed, and the removal rate was about 10.1%; there was no discharge phenomenon in 7.5 mm discharge gap reactor. The voltage continued increasing until NO removal rate approached 100%. Voltage and current waveforms were acquired by oscilloscope (Fig.6), while the corresponding removal rates and voltages were recorded, and according to waveform data, reactor's discharge powers can be calculated based on instantaneous law.

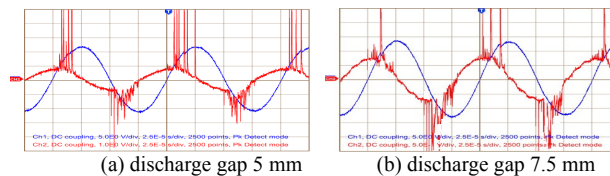


Figure 6. Applied voltage and total current waveforms

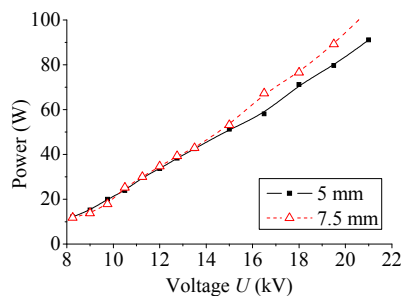


Figure 7. Discharge power as a function of applied voltage

Voltage and current waveforms shown in Fig. 6 presented discharge gap 5 mm had more severe discharge, and that was the narrow gap discharge intensely. This is because, when the discharge gap increased from 5 mm to 7.5 mm, the capacitor of discharge gap decreased and the discharge starting voltage increased, thereby all of them affected the effective discharge time [8]. Meanwhile, because cross-sectional area of the discharge gap increased with the gap, the gas residence time within the discharge tube extended. As the gap enlarged, the number of micro-discharge channel reduced, the distribution of channels became increasingly inhomogeneous, each micro-discharge channel turned thick, and the energy distribution of plasma generated was more concentrated. When input voltage remained unchanged, discharge power declined slightly as gap increased. Fig. 7 showed the evolution of the discharge power as a function of the applied voltage at different discharge gaps. When the voltage was less than 12 kV, the larger discharge gap is the power smaller, but when the voltage was greater than 12 kV, with the supply voltage increased, the power of 7.5 mm discharge gap was larger. This was because when the space was large, high energy electrons in the discharge space had sufficient time and space to collide with other gas atoms or molecules and then large area electron avalanche phenomenon occurred, so power consumption was relatively large.

Therefore, if other parameters do not change, select the appropriate discharge gap; you can make the best NO removal efficiency. Taking the stability of discharge and parameters of the broad tuning range into account, it will be better to choose $\Phi 20 \times \Phi 16 + \Phi 6 \times \Phi 4$ reactor in subsequent experiments.

5.4 Effect of power voltage on removal rate of NO

It is found that voltage and frequency are very important factors that affect the discharge [9]. In the experiment, regulate voltage by the regulator and maintain frequency by Plasma power frequency adjustment knob, use a reactor discharge gap of 5mm applied voltage on NO removal rate. We can see from Fig. 8, with the voltage increases, NO removal rate increased from 11.7% to 95.8%, during the process that voltage increases from 6.9 kV to 11.25 kV, the removal rate increased almost linearly, after that, increasing trend gradually decrease with the voltage increase.

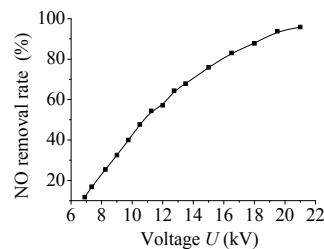


Figure 8. Relation between removal rate of NO and supply voltage

The result shows that with voltage increasing, NO removal rate increases. This is because the voltage increases when the discharge power increases with the increasing density of electrons to high energy per unit area increase in the number of micro-discharge, discharge more and more intense, accelerated NO removal. The same time, the experiment can also see that there is no voltage below 6.5 kV discharge phenomenon, NO concentrations remained unchanged, and when the voltage exceeds 6.9 kV NO removal occurs after the jump. This is because when the energy of the particles to achieve effective chemical reaction occurs before the particles of energy are used for changing the rotational energy, which has its discharge reaction, "Starting voltage" [10]. Numerical simulation results also show that [11], although the applied voltage in a larger context of change, but the discharge time of the space charge shielding effect, electric field strength within the discharge gap remained unchanged, that is, the voltage change on the high-energy electron number density no significant impact. However, changes in the alternating voltage cycle, not all discharge, only when the applied voltage reaches the start only when the breakdown voltage discharge, and when the applied voltage reaches the peak voltage, the discharge end. Thus in one cycle, sometimes, NO removal reaction occurs. When the applied voltage increases, discharge time can extend effectively and the NO removal rate also increases.

5.5 Effect of power frequency on removal rate of NO

NO removal rate and power frequency are not simple linear relationship, but as power frequency increasing, the removal rate of NO increased first and then decreased [12, 13]. To study effect of power frequency on NO removal, adjust power frequency from 5 kHz to 11 kHz at voltage is 11.2 kV without changing other reaction parameters. NO removal rate and power frequency relationship is shown in Fig. 9.

Increasing frequency reduces the discharge starting voltage, and can make discharge more uniform and stable. With the increase of power frequency, into the reactor per unit time increase in the number of electronic, was making more obvious effect of NO removal. However, the increase of frequency will lead to increased power consumption of energy; the energy injected into the reactor has decreased, affecting the removal efficiency.

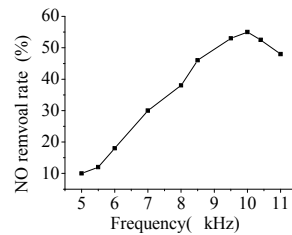


Figure 9. Relation between NO removal rate and frequency

This can be explained by the theory of series resonant [14]. As shown in Fig. 1, the dielectric barrier discharge equivalent circuit was resistive, when series resonance occurred. At this time, the circuit impedance was minimum, current was maximum, and reactor terminal voltage can be many times greater than the total voltage. The essential condition of series resonance circuit was $\omega L = 1/\omega C$, while resonance frequency was $f_0 = 1/2\pi\sqrt{LC}$. When the frequency was lower, micro discharge only occurred in local space, so the impedance of discharge space was very large. With frequency increasing, resonance would occur. When frequency was less than the resonant frequency, capacitance and inductance increased with increasing frequency, so that the total electrical resistance increased but was less than zero, leading to resistance decreased and current increased. When the frequency is higher than the resonant frequency, with frequency increasing, the total reactance continued to increase, leading to inductance increased and discharge current decreased rapidly. The number of micro-discharge in space significantly reduced until disappeared, and resistance formed in discharge space significant increased until insulation. When power frequency was equal to the resonant frequency, the total reactance was zero, impedance was a minimum, almost all of the power energy was available to the resistance load, at this moment NO removal rate should be the highest. According to this theory the trend curve in Fig. 9 may be explained, and the resonant frequency of reactor can be confirmed which was about 10 kHz.

6. Conclusions

With the increase of the length of the discharging area of the reactor, the removal rate of NO raises. But the length has little influence on the change of the removal rate. Thus, from economic point of view, an appropriate length can be chosen.

When other parameters of reactor remain unchanged, removal rate of NO increased at first and then decreased with the discharge gap increasing. Considering the stability of discharge and the universality of regulation parameters, there is an optimal discharge gap value.

Supply voltage has significant effect on NO removal efficiency. The higher the voltage is, the greater the removal rate is. In the initial stage, the removal rate increases rapidly with the increasing voltage, but as the voltage continues rising, the growth trend will slow down.

Keeping the supply voltage unchanged, with the increase of power frequency, the removal rate of NO increases at first and then decreases. For a given power supply and reactor, one can adjust the frequency to find a best one. If, as the increase of the frequency, the removal rate keeps increasing, it proves that the resonant frequency of the circuit consists of the power supply and the reactor is greater than the maximum frequency of the power supply; otherwise, lower.

7. Acknowledgment

This work is supported by “the Fundamental Research Funds for the Central Universities” (09ZG02), and supported by Program for Changjiang Scholars and Innovative Research Team in University (PCSIRT0720).

8. References

- [1] Xue-Ji Xu and Ding-Chang Zhu, *Gas Discharge Physics* [M]. Shanghai: Fudan Press, 1996.
- [2] B. Eliasson, and U. Kogelschatz, “Modeling and applications of silent discharge plasmas,” *IEEE Transactions on Plasma Science*, vol. 19(2), pp. 309–323, April 1991.
- [3] B. Eliasson, M. Hirth, and U. Kogelschatz, “Ozone synthesis from oxygen in dielectric barrier discharges,” *J. Phys D: Appl. Phys.*, vol. 20(11), pp. 1421–1437, 1987.
- [4] B. Pashaie, R. Sankaranarayanan, and S. K. Dhali, “Experimental investigation of microdischarges in a dielectric-barrier discharge,” *IEEE Transactions on Plasma Science*, vol. 27(1), pp. 22–23, 1999.
- [5] Xin-xin Wang, Ming-ze Lu, and Yi-kang Pu, “Possibility of atmospheric pressure glow discharge in air,” *ACTA PHYSICA SINICA*, vol. 51 (12), pp. 2778–2785, Dec. 2002.
- [6] Xu-dong Zhang, “Studies on the NO Removal with the Dielectric Barrier Discharges Non-thermal Plasma [D],” Beijing: Dep. Engineering Mechanics, Tsinghua University, 2003.
- [7] Wen-hua Zhao, and Xu-dong Zhang, “Influence of discharge reactor design on the NO removal rate with dielectric barrier discharges,” *J. Tsinghua Univ: Sci & Tech*, vol. 43(11), pp. 1515–1518, 2003.
- [8] K. Yukimura, K. Kawamura, S. Kambara, H. Moritomi and T. Yamashita, “Correlation of Energy Efficiency of NO Removal by Intermittent DBD Radical Injection Method,” *IEEE Trans. Plasma Science*, vol. 33, pp. 763–770, 2005.
- [9] H.R. Snyder, G.K. Anderson, “Effect of air and oxygen content on the dielectric barrier discharge decomposition of chlorobenzene,” *IEEE Trans. on Plasma Science*, vol. 26(6), pp. 1695–1699, 1998.
- [10] C.R. McLarnon, and V.K. Mathur, “Nitrogen oxide decomposition by barrier discharge,” *Ind. Eng. Chem. Res.*, vol.39(8), pp. 2779–2787, 2000.
- [11] B.M. Penefante, M.C. Hsiao, and etal., “Comparison of electrical discharge techniques for non-thermal plasma processing of NO in N₂,” *IEEE Trans. on Plasma Science*, vol. 23(4), pp. 679–687, 1995.
- [12] Tao Zhu, Jian Li, Wen-jun Liang, and etal., “Experimental research on toluene decomposition with high frequency DBD,” *High Voltage Engineering*, vol. 26 (5), pp. 359–363, 2009.
- [13] Bo Zhou, Wen-feng Lin, and etal., “Kinetic simulation of NO/O₂/N₂/Hg streamer under dielectric barrier discharge,” *J. Engineering Thermophysics*, vol. 30(20), pp. 333–346, 2009.
- [14] C.M. Nunez, G.H. Ramsey and etal., “Corona destruction: An innovative control technology for VOCS and air toxics,” *Air and Waste Management Association*, vol. 43, pp. 242–247, 1993.